Investigation on extraction rate of lanthanides with extractant-impregnated microcapsule

Eiji Kamio [a], Yasuhide Fujiwara [b], Michiaki Matsumoto [b], Fernando Valenzuela [c], Kazuo Kondo [b,*]

[a] *Department of Environmental Chemistry and Materials, Okayama University, 3-1-1 Tsushima-naka, Okayama-shi, Okayama 700-8530, Japan*
[b] *Department of Chemical Engineering and Materials Science, Doshisha University, Kyotanabe, Kyoto 610-0321, Japan*
[c] *Faculty of Chemical and Pharmaceutical Sciences, Chile University, P.O. Box 233, Santiago, Chile*

Abstract

Extraction of lanthanum, samarium and erbium into a microcapsule containing 2-ethylhexylphosphonic acid mono-2-ethylhexyl ester (EHPNA) is studied. The extraction kinetic model used to predict uptake curves is based on the interfacial reaction model accompanied by intraparticle diffusion expressed by Fick's law. The uptakes are analyzed using the kinetic model with the separately determined complex formation rate constants and the intraparticle diffusion coefficient. The rate constants used in the calculation are determined from the analysis of the kinetics data for the liquid–liquid extraction system under a low-extractant concentration. The effects of pH and metal concentration on the metal uptakes into the microcapsule are successfully predicted with the determined rate constants. From the results, it is confirmed that the extraction mechanism of metal ions into the microcapsule is same to that for a liquid–liquid extraction system.

1. Introduction

Over the last few decades, efficient separation of lanthanoids has been studied actively in connection with the development of new, advanced materials that utilize their superior properties. Conventional liquid–liquid extraction is a well-known effective method for separation and concentration of lanthanoids on an industrial scale. However, the process requires a large number of stages in a series of mixer-settlers to prepare products of high purity, because the chemical and physical properties of adjacent elements are very similar among the lanthanoids.

Since the invention of polymeric adsorbents impregnated with liquid ligands by Small [1], separation of metal ions using polymeric adsorbents impregnated with a liquid extractant has been noted as a novel method for separating and concentrating metal ions. This process is capable of giving a higher degree of concentration of metal ions in fewer stages, while maintaining the high selectivity of the extractant used in the liquid–liquid extraction process. In general, two forms of polymeric support geometry are used, so-called solvent-impregnated resins (hereafter referred to as SIRs) and microcapsules. Impregnation of an extractant into SIRs and microencapsulation of extractant has several advantages: prevention of extracant loss, protection of an extractant against outer environments and easy handling as powder-like materials. Most extractants which are generally used for current industrial processes can be easily enclosed in SIRs and microcapsules. We can select an adequate extractant which has great selectivity for the target metals. For SIRs, several papers have been presented on the recovery and separation of lanthanoids [2–12], however, there are very few papers concerning microcapsules. Only a few groups have reported on the extraction and separation of lanthanoids by microcapsules. Nishihama et al. studied the extraction and separation of lanthanoids such as Pr^{3+}, Nd^{3+}, Sm^{3+}, Er^{3+} and Y^{3+} by using microcapsules containing bis-(2-ethylhexyl)phosphoric acid [13]. We reported the extraction equilibria of Y^{3+}, light rare earth elements such as La^{3+}, Ce^{3+} and Pr^{3+}, middle rare earth elements such as Sm^{3+}, Eu^{3+} and Gd^{3+} and heavy rare earth elements such as Ho^{3+} and Er^{3+} with organophosphorus extractant-impregnated microcapsules [14]. In that paper, we also reported the separation and concentration of rare earth elements present in the same sample. However, there has been no

* Corresponding author. Tel.: +81 774 65 6656; fax: +81 774 65 6656.
 E-mail address: kkondo@mail.doshisha.ac.jp (K. Kondo).

Nomenclature

A	interfacial area between aqueous phase and organic phase (m^2)
A_{MC}	effective surface area of microcapsules packed in shallow bed (m^2)
b	molecular number of extractant bonding with a metal element
D_{com}	diffusion coefficient of extracted complex in liquid organic laminar film (m^2/s)
E	extent of metal extracted
$E_{HR,org}$	$[HR]_{ad}/[HR]_{org,i}$
$F(t)$	fractional attainment of equilibrium of metal extraction
i	ionic valence of counteranion
I	Souders viscosity constant
j	association degree of extracted complex
k	general constant
k_{com}	mass transfer coefficient of extracted complex across organic laminar film (m/s)
k_I	apparent rate constant of complex formation (m^3/(mol s))
k_M	mass transfer coefficient of metal ion across aqueous laminar film (m/s)
k_1	complex formation rate constant between metal ion and EHPNA monomer (m^3/(mol s))
k_2	complex formation rate constant between metal ion and anionic species of EHPNA (m^3/(mol s))
K	Langmuir constant (m^3/mol)
K_a	distribution constant of extractant between aqueous and organic phases
K_D	distribution coefficient of EHPNA
$K_{ex,SX}$	extraction equilibrium constant ($(mol/m^3)^{(3-x)/2}$)
$K_{ex,1}$	extraction equilibrium constant at low loading
$K_{ex,2}$	extraction equilibrium constant at high loading ($(mol/m^3)^{0.5}$)
K_2	dimerization constant of EHPNA (m^3/mol)
$K^*_{HR,org}$	adsorption equilibrium constant of EHPNA on the interface (m^3/mol)
m	weight of microcapsules (g)
M_1	molecular weight of EHPNA
M_2	molecular weight of n-heptane
n	in Eq. (18) a positive number
n	ionic valence of metal cation
q	amount of metal extracted in unit mass of microcapsules (mol/g MC)
q_∞	saturation amount of metal extracted in microcapsules (mol/g MC)
q^*	equilibrium extraction amount of metal in microcapsules (mol/g MC)
$Q\|_{r=r}$	concentration of extracted complex at a certain point in radius direction (mol/m^3)
r	radius distance in a microcapsule (m)
r_I	formation rate of extracted complex (mol/(m^3 s))
r_0	radius of a microcapsule (m)

R_{aq}	mass transfer rate of $MB^{(n-i)+}$ through liquid aqueous laminar film (mol/(m^2 s))
R_i	complex formation rate of $MB^{(n-i)+}$ and EHPNA (mol/(m^2 s))
R_{org}	mass transfer rate of extracted complex through liquid organic laminar film (mol/(m^2 s))
R_0	overall initial extraction rate (mol/(m^2 s))
t	time (s)
T	temperature (K)
V_{aq}	volume of aqueous phase in the stirred transfer cell (m^3)
$V_{org,MC}$	volume of EHPNA in unit mass of microcapsules (m^3)
V_1	molecular volume of EHPNA (m^3)
x	solvation number of EHPNA in extracted complex
x_1	molar ratio of EHPNA
x_2	molar ratio of n-heptane

Greek letters

Γ	adsorption excess of EHPNA (mol/m^2)
Γ^∞	saturation adsorption amount of EHPNA (mol/m^2)
δ_2	zone thickness of interface between aqueous and organic phases (m)
δ_3	liquid organic laminar film thickness (m)
ε_{MC}	pore density of a microcapsule
η	viscosity of organic phase (mPa s)
ρ_m	density of organic phase (g/m^3)
ρ_{MC}	weight of microcapsules per unit volume (g/m^3)
$\phi(t)$	extracted complex concentration at surface of a microcapsule (mol/m^3)
ψ	association constant of solvent

Subscripts

ad	chemical species adsorbing on liquid–liquid interface
aq	aqueous phase
com	metal–EHPNA complex
HR	EHPNA monomer
i	interface between aqueous and organic phases
MC	microcapsule system
org	organic phase
R–	acid-dissociated EHPNA monomer
SX	liquid–liquid extraction system
0	initial state

investigation on extraction kinetics of lanthanoids by SIRs as well as microcapsules. In order to design an extraction process, knowledge of kinetic data is important.

Because SIRs and microcapsules would act as powder-like adsorbents containing a liquid extractant, they would exhibit the characteristics of both an ion-exchange resin and an extractant used in a liquid–liquid extraction system. It was suggested that a complex formation reaction at the surface as well as

intraparticle diffusion of the extracted complex would occur during metal extraction with SIRs and microcapsules [15]. Recently, we developed a theoretical model to describe an uptake curve of gallium and indium with a microcapsule containing 2-ethylhexylphosphonic acid mono-2-ethylhexyl ester (hereafter written as EHPNA) [16]. In the model we developed, both of the processes concerned with the rate-determining step of extraction were considered. Using the proposed model, we carried out the detailed investigation on the extraction dynamics of gallium and indium into the microcapsule containing EHPNA in the previous papers. The main purpose of the previous papers was to elucidate the extraction mechanism of metals into the microcapsule. As the result, we elucidated the extraction mechanism. In addition to attain the object of the previous studies, we determined the parameters used for the analysis of extraction dynamics of the metals into the microcapsule under peculiar and extreme condition. That is to say, we determined the rate constants from the experiments using undiluted extractant for the liquid–liquid extraction system. However, the liquid–liquid extraction process is usually operated using organic phase containing an extractant in low concentration. Therefore, if we can use the kinetic parameters determined from the liquid–liquid extraction under usual condition in order to predict the extraction behavior for the microcapsule system, the proposed kinetic model for microcapsule extraction becomes more useful in practice.

In the present study, the extraction dynamics of La^{3+}, Sm^{3+} and Er^{3+} were investigated by using microcapsules containing EHPNA as an extractant along with measurement of their extraction dynamics using a liquid–liquid extraction system. The main purpose of the present study is to indicate that the extraction behavior of metal ions into the microcapsule can be well explained by using the rate constants determined from the liquid–liquid extraction system under usual condition. As we reported in the previous paper, it is considered that the extraction mechanism of metals for the microcapsule system is the same as that for the liquid–liquid extraction system. Therefore, it is expected that the extraction behavior for the microcapsule system would be predicted with the rate constants determined from the usual liquid–liquid extraction system. However, it is just an expectation; i.e. there is no investigation on the prediction of metal uptakes for the microcapsule system using the rate constants determined for the usual liquid–liquid extraction system. It is still unclear whether the uptakes for the microcapsule system successfully predicted with the rate constants determined for the usual liquid–liquid extraction system or not. Thus, in the present study, we determined the rate constant of metal extraction for the usual liquid–liquid extraction system, and predicted the uptake curves of lanthanides for the microcapsule system by using the determined rate constants.

2. Experimental

2.1. Reagents

EHPNA was kindly supplied by Daihachi Chemical Industry Co. Ltd., Osaka, and was used without further purification. Microcapsules containing EHPNA as an extractant were prepared by the same procedure as described elsewhere [17]. A mixture of divinylbenzene, toluene, N,N'-azobis(2,4-dimethylvaleronitrile) and EHPNA were used as a dispersed phase and an aqueous solution containing gum-arabic was used as a continuous phase. The disperse phase was poured into the continuous phase which was agitated at 300 rpm, and O/W emulsion was prepared. The oily droplet was polymerized at 343 K for 6 h to prepare the microcapsule.

An appropriate amount of $LaCl_3$, $SmCl_3$ or $ErCl_3$ was dissolved in 100 mol/m³ $(H,Na)_2SO_4$ aqueous solution. The pH of the aqueous solution was adjusted with a pH meter (Horiba F-23).

2.2. Extraction isotherms of lanthanides extracted with microcapsules

The extraction isotherms of lanthanum, samarium and erbium were measured under batch conditions. Aqueous solutions containing various metal concentrations and 0.1 g of the microcapsules were contacted for over 86.4 ks to attain equilibrium. The metal concentration in the aqueous solutions was then measured by inductively coupled plasma spectrometry (ICP-AES, Shimadzu ICPS-8000). The amount of metal extracted into the microcapsule was determined by mass balance before and after equilibrium.

2.3. Extraction rates of lanthanides into microcapsules

Considering that the microcapsules containing EHPNA exhibit strong hydrophobicity at pH < 4 and are not ideally dispersed on mixing, we measured the kinetic data using the shallow bed method. The shallow bed apparatus used is the same as that presented in the previous paper [16]. 0.05 g of the microcapsules was packed into the bed, their physical properties were as shown in Table 1. The bed was conditioned by feeding with a conditioning solution without lanthanide ions for 1.8 ks. After 1.8 ks, a feed solution containing the desired amount of lanthanum, samarium or erbium ions was passed through the bed for appropriate periods. It was found in the preliminary experiments that a flow rate of 1.167×10^{-6} m³/s was sufficient for ignoring the liquid film diffusion resistance surrounding the microcapsules. As soon as the desired time had passed, a scrubbing solution was introduced into the bed at a fast flow rate to remove the feed solution remaining in the bed. Two minutes were enough to completely remove the feed solution remaining in the bed. The obtained microcapsules were then collected and contacted with the stripping solution for over 8.64×10^4 s. The stripping agent was 2×10^3 mol/m³ H_2SO_4 solution, because 2×10^3 mol/m³

Table 1
Physical properties of the microcapsule containing EHPNA

Amount of EHPNA, $q_{HR,MC}$	1.6×10^{-3} mol/g MC
Average radius, r_0	7.5×10^{-5} m
Porosity, ε_{MC}	5.2×10^{-1}
Density, ρ_{MC}	9.9×10^5 g/m³ MC
Surface area, A_{MC}	0.054 m²/g MC

Table 2
Standard experimental condition for kinetic experiment

Standard experimental condition for microcapsule system	
Flow rate	1.167×10^{-6} m^3/s
Reynolds number of feed solution	3870
Microcapsules packed	0.05 g
pH of the conditioning and feed solution	2.2 for lanthanum and samarium; 1.5 for erbium
Metal concentration in the bulk	0.5 mol/m^3
[SO$_4$]$_{total}$	100 mol/m^3
pH of the scrubbing solution	3.5 for lanthanum; 3.0 for samarium and erbium
Stripping solution	2.0×10^3 mol/m^3 H$_2$SO$_4$
Temperature	313 K
Standard experimental condition for liquid–liquid extraction system	
Stirring speed	8.4 s^{-1}
Volume of the aqueous phase	1.36×10^{-4} m^3
Volume of the organic phase	1.36×10^{-4} m^3
pH of the aqueous phase	3.0 for lanthanum; 2.2 for samarium and erbium
Metal concentration in the aqueous phase	0.4 mol/m^3 for lanthanum; 0.5 mol/m^3 for samarium and erbium
EHPNA concentration in the organic phase	100 mol/m^3
Temperature	313 K

H$_2$SO$_4$ solution can completely strip the metals extracted in a microcapsule. The metal concentration in the stripping solution was measured by ICP-AES. The standard experimental conditions are described in Table 2. The metal concentration or the pH of the aqueous solution was varied for each experiment. All experiments were carried out at 313 K, because we had observed in the previous investigations that larger amounts of metal–EHPNA aggregates were formed at 303 K compared with the experiment performed at 313 K. The formation of the metal–EHPNA aggregates incurs undesirable fall in extraction rate. That is why we carried out the experiments at 313 K.

2.4. Extraction equilibria of lanthanides in a liquid–liquid extraction system at a high EHPNA concentration

An aqueous phase containing an appropriate concentration of each lanthanide ion and an organic phase containing an appropriate concentration of EHPNA were mixed in a stoppered flask and dispersed homogeneously by ultrasonication for 1.2 ks. They were then shaken in a thermostatic bath at 313 K for 3.6 ks for equilibration. After that, they were stood in a thermostatic bath at 313 K for 21.6 ks to separate the two phases. The resultant aqueous phase was collected and centrifuged for 1.2 ks at 240 s^{-1} to completely remove any remaining organic phase. The metal concentration in the resultant aqueous solution was measured by using ICP-AES. The metal concentration extracted into the organic phase was calculated from the mass balance before and after equilibrium.

2.5. Kinetics experiment for liquid–liquid extraction system

A stirred transfer cell [18] was used to measure the extraction rates of lanthanum, samarium and erbium by EHPNA. The

solutions in the cell were stirred at 8.4 s^{-1} since it was found in preliminary experiments that this stirring speed is fast enough to overwhelm the liquid film diffusion resistance. Aqueous solutions containing no lanthanide ions and n-heptane containing 100 mol/m^3 of EHPNA were introduced into the lower compartment and higher compartment, respectively. The stock solution containing the lanthanide ion was then introduced into the aqueous phase in the lower compartment. Small volume samples were taken at intervals from the aqueous phase. The metal concentration in these samples was measured by ICP-AES. The standard experimental conditions are described in Table 2. The metal concentration and pH of the aqueous phase were varied for each experiment. All experiments were carried out at 313 K.

3. Theoretical section

3.1. Interfacial reaction model

Before prediction of uptake curves resulting from the extraction with the microcapsule, the key parameters such as complex formation rate constants and intraparticle diffusion coefficient were determined from the liquid–liquid extraction under a low-extractant concentration. The parameters were determined from the analysis of the experimental data for liquid–liquid extraction with the interfacial reaction model described below.

Metal ions form complexes with coexisting anionic ions in an aqueous phase and exist as a variety of cationic species. The n-valent cationic metal species which have to be considered in this study are mainly the following three types: MSO$_4^{(n-2)+}$, M^{n+} and MOH$^{(n-1)+}$. The i-valent anionic species are written as B^{i-}. The overall extraction process in liquid–liquid extraction system consists of the following three steps: (I) mass transfer of cationic metal species, MB$^{(n-i)+}$, from the aqueous bulk to the interface between the aqueous and organic phases, (II) a complex formation reaction of MB$^{(n-i)+}$ with extractant at the interface, and (III) mass transfer of the formed extracted complex from the interface to the organic bulk. Therefore, the overall extraction rate, R_0 is expressed as

$$R_0 = \frac{1}{R_{aq}^{-1} + R_i^{-1} + R_{org}^{-1}} \tag{1}$$

where R_{aq}^{-1}, R_i^{-1} and R_{org}^{-1} express the resistances of each step, respectively [19]. Therefore, it is necessary to consider in detail these three steps. The mathematical expression of R_{aq}^{-1}, R_i^{-1} and R_{org}^{-1} are written as follows.

3.1.1. Mass transfer of MB$^{(n-i)+}$ to the interface between the aqueous and organic phases across the aqueous film

When MB$^{(n-i)+}$ diffuses through the aqueous film according to a linear driving force approximation from the aqueous bulk to the interface, the mass transfer resistance is expressed by the mass transfer coefficient of MB$^{(n-i)+}$, k_M, as follows:

$$R_{aq}^{-1} = (k_M[MB^{(n-i)+}]_{aq})^{-1} \tag{2}$$

where $[MB^{(n-1)+}]$ denotes the concentration of cationic metal species which takes part in the extraction. They were calculated by using the stability constants for their complex formation equilibria.

3.1.2. Complex formation reaction between $MB^{(n-i)+}$ and the extractant at the interface

It is considered that the reaction field of complex formation when using EHPNA as the extractant is the interface between the aqueous and organic phases, because EHPNA adsorbs on the liquid–liquid interface. Thus, the resistance of the complex formation reaction at the interface is written as

$$R_i^{-1} = \left(\frac{r_I}{2}\delta_2\right)^{-1} \tag{3}$$

where r_I is the formation rate of extracted complex, $(MR_n xHR)_j$, and δ_2 the zone thickness of the interface which corresponds to the molecular length of EHPNA adsorbed on the interface. In addition, in Eq. (3), we take the steric angle of the interfacial reaction field compared to the bulk into consideration as 1/2.

Here, we consider r_I. At the interface, the formation reaction of an extracted complex takes place sequentially. The rate-determining step of the sequential reaction is considered to be the formation of an intermediate complex of $MR^{(n-1)+}$. Thus r_I can be expressed as the following rate equation:

$$r_I = k_1[HR]_{ad}[MB^{(n-i)+}]_{aq,i} + k_2[R^-]_{ad}[MB^{(n-i)+}]_{aq,i} \tag{4}$$

where k_1 is the complex formation rate constant between the metal ion and the EHPNA monomer and k_2 is that between the metal ion and the acid-dissociated EHPNA monomer. In Eq. (4), reverse reactions are not taken into consideration, because they can be ignored during the initial periods of extraction. HR and R^- represent EHPNA and its anionic form, respectively. The subscripts ad and i represent the chemical species adsorbed on the interface and that existing in the aqueous phase near the interface, respectively. The concentration of extractant at the interface is written as the adsorption excess of EHPNA, Γ, as follows:

$$[HR]_{ad} = [HR]_{org,i} + \frac{\Gamma_{HR,org}}{\delta_2},$$

$$[R^-]_{ad} = [R^-]_{aq,i} + \frac{\Gamma_{R^-,aq}}{\delta_2} \tag{5}$$

By using Eq. (5) and considering the physico-chemical properties of EHPNA such as the acid dissociation, the distribution between the aqueous and organic phases and the dimerization equilibrium, Eq. (4) can be transformed to the following equation [18,19]:

$$r_I = k_I[HR]_{org,i}[MB^{(n-i)+}]_{aq,i} \tag{6}$$

$$k_I = k_1 E_{HR,org} + \frac{k_2\{K_D(E_{HR,org} - 1) + 1\}K_a}{K_D[H^+]} \tag{7}$$

where K_D and K_a are the distribution coefficient and acid dissociation constant of EHPNA, respectively. $E_{HR,org}$ is the ratio of

extractant concentration at the interface to that in the bulk:

$$E_{HR,org} = 1 + \frac{\Gamma_{HR,org}^\infty K_{HR,org}^*}{\delta_2(1 + K_{HR,org}^*(1 + (K_a/[H^+]))[HR]_{org,i})} \tag{8}$$

where $K_{HR,org}^*$ and $\Gamma_{HR,org}^\infty$ are adsorption equilibrium constant and saturation adsorption amount of EHPNA on the interface, respectively. They were determined from the analysis of the relationship between interfacial tension of EHPNA and EHPNA concentration [18].

Using Eq. (6), the complex formation resistance, R_i^{-1} is rewritten as follows:

$$R_i^{-1} = \left(\frac{k_I[HR]_{org,i}[MB^{(n-i)+}]_{aq,i}}{2}\delta_2\right)^{-1} \tag{9}$$

3.1.3. Mass transfer of extracted complex from the interface to the organic bulk across the organic film

When $(MR_n xHR)_j$ diffuses through the organic film according to a linear driving force approximation, the mass transfer resistance is expressed as the following equation:

$$R_{org}^{-1} = (k_{com}[(MR_n xHR)_j]_{org})^{-1} \tag{10}$$

where k_{com} is the mass transfer coefficient of $(MR_n xHR)_j$. The constants j and x are the degree of association of the complex and the solvation number of EHPNA, respectively.

Assuming local equilibrium of the complex formation reaction near the interface, Eq. (10) is rewritten as follows:

$$R_{org}^{-1} = \frac{k_{com}K_{ex,SX}[M]_{aq,0}^j[(HR)_2]_{org}^{j(n+x)/2}}{K_{ex,SX}[(HR)_2]_{org}^{j(n+x)/2} + [H^+]^{jn}} \tag{11}$$

where $K_{ex,SX}$ is the extraction equilibrium constant. In addition, the mass transfer coefficient of the extracted complex is expressed by using the diffusion coefficient, D_{com}, as follows:

$$k_{com} = \frac{D_{com}}{\delta_3} \tag{12}$$

where δ_3 is the organic film thickness. In the interfacial reaction model, D_{com} is expressed as a function of the extractant concentration. D_{com} is a function of the viscosity of the solution, η, which can be expressed by the following Wilke–Chang equation [20]:

$$D_{com} = 7.4 \times 10^{-12}\frac{\sqrt{\psi M}T}{\eta V_1^{0.6}} \tag{13}$$

where ψ and M are the association parameter and the molecular weight of solvent, respectively. As reported by Wilke and Chang [20], the association parameter of unassociated solvent such as n-heptane is 1, and that of associated solvent is greater than 1. Because n-heptane was used as a solvent for the liquid–liquid extraction system under a low EHPNA concentration, $\psi = 1$ was used in the calculation for liquid–liquid extraction system. On the other hand, EHPNA exists as undiluted state and act as a solvent in the microcapsule. EHPNA generally associates with each other in non-polar solvent and forms dimer. Therefore, we

assumed that $\psi = 2$ for the microcapsule system. T is temperature. V_1 is the molecular volume of EHPNA calculated from its atomic volumes [21]. In Eq. (13), the viscosity of the solution can be expressed by the equation proposed by Lima as follows [22]:

$$\log(\log \eta \times 10) = \frac{(x_1 I_1 + x_2 I_2)\rho_m}{x_1 M_1 + x_2 M_2} - k \tag{14}$$

where subscripts 1 and 2 mean the extractant (EHPNA) and solvent (n-heptane), respectively. ρ_m is the density of the organic solution and x is the molar ratio, which are a function of the concentration. I and k are the Souders viscosity constant and a general constant, respectively. By using Eqs. (13) and (14), we determined the diffusivity of extracted complex in the organic phase under both conditions of low EHPNA concentration and undiluted EHPNA. The suitability for using Wilke–Chang equation for the undiluted EHPNA system is shown below.

Wilke–Chang equation was proposed to estimate the diffusivity of solute in diluted solution. They reported the diffusivity of many different solutes in low viscose solutions [20]. On the other hand, Chang and Wilke also reported the diffusivity of solute in high viscous solvent-like ethylene glycol [23]. In the undiluted EHPNA system as well as the microcapsule system, the extracted complex is diffusive solute and EHPNA is a solvent. These systems are regarded as a dilute system, because the concentration of extracted complex is quite low compared with EHPNA. Regarding the viscosity, we compared the viscosity and diffusivity calculated for our system with those of solutes in high viscous solvent (ethylene glycol) which was reported by Chang and Wilke [23]. The diffusivities are summarized in Table 3. As shown in Table 3, the calculated diffusivities were almost the same as the reported value in the solvent with nearly same viscosity. This indicates that Wilke–Chang equation is useful to estimate the diffusivity of extracted complex in undiluted EHPNA.

Therefore, by using Eqs. (12)–(14), R_{org}^{-1} can be expressed as a function of the extractant concentration in the organic phase.

3.2. Kinetic model for extraction with microcapsule

The overall extraction mechanism considering in the theoretical model for microcapsule extraction is the stepwise process of the following two steps: (I) complex formation reaction at the liquid–liquid interface and (II) intraparticle diffusion of the extracted complex toward the center of the microcapsule through the pores. First, we consider the kinetic description of the complex formation reaction according to the above mentioned interfacial reaction model. We adapted Eq. (9) in order to express the complex formation reaction for the microcapsule system [16]:

$$
\begin{aligned}
R_0 &= -\frac{V_{org,MC}}{bA_{MC}} \left. \frac{d[HR]_{org,total}}{dt} \right|_{t=0} \\
&= \frac{k_I [HR]_{org,i} [MB^{(n-i)+}]_{aq,i} \delta_2}{2}
\end{aligned} \tag{15}
$$

where R_0 is the initial rate of extraction. $V_{org,MC}$ is the volume of EHPNA in a unit mass of microcapsules. The $V_{org,MC}$ was calculated from the relationship; $V_{org,MC} = q_{HR,MC} M_{HR}/\rho_{HR}$ where M_{HR} and ρ_{HR} are the molecular weight and density of EHPNA, respectively. A_{MC} is the effective surface area of a unit mass of microcapsules. In this study, A_{MC} is calculated as the spherical surface area with r_0 as its radius, because it can be regarded that EHPNA reacts with a metal ion at the surface of a microcapsule. b denotes the number of EHPNA molecules contributing to the complex formation in one molecule of the extracted complex and t is the time.

From the mass balance of EHPNA, the extracted complex concentration at an arbitrary point in the reaction, $[MR_3]_{org,i}$, is expressed as the following equation [16]:

$$
\begin{aligned}
&[MR_3]_{org,i} \\
&= -\frac{-[HR]_{org,total} + e^{\alpha\beta t}[HR]_{org,i,0} + 2K_2 e^{2\alpha\beta t}[HR]_{org,i,0}^2}{b}
\end{aligned} \tag{16}
$$

where $\alpha = -\frac{\Gamma_{HR,org}^{\infty} K_{HR,org}^{*}}{4\delta_2}\left(k_1 + \frac{k_2 K_a}{[H^+]}\right)$ and $\beta = \frac{1}{2}\frac{bA_{MC}}{V_{org,MC}}\frac{[MB^{(n-i)+}]_{aq,i}\delta_2}{1078}$ and K_2 is dimerization constant of EHPNA.

Subsequently, we will consider intraparticle diffusion of the extracted complex into a microcapsule with radius r_0. The nonsteady diffusion equation for the radial diffusion with a constant intraparticle diffusion coefficient, D_{com}, is as follows:

$$\frac{D_{com}}{r^2}\frac{\partial}{\partial r}\left(r^2 \frac{\partial[MR_3]_{org,i}}{\partial r}\right) = \frac{\partial[MR_3]_{org,i}}{\partial t} \tag{17}$$

Integrating Eq. (17) under the initial condition ($[MR_3]_{org,i} r = 0$ at $t = 0$) and boundary conditions ($[MR_3]_{org,i} r = 0$ at $r = 0$ and $[MR_3]_{org,i} r = r_0 \phi(t)$ at $r = r_0$), the concentration of extracted complex at a position r in the direction of the radius, $Q|_{r=r}$,

Table 3
Relationships between viscosity of solution and diffusivity

Condition	Extracted complex		Acetic acid 288 K (solvent: ethylene glycol [23])	Formic acid 323 K (solvent: ethylene glycol [23])
	Solvent: EHPNA 3100 mol/m³	Solvent: EHPNA 2900 mol/m³		
Viscosity of solution (mPa s)	33.9[a]	6.62[a]	26	6.62
Diffusivity, D_{com} (cm²/s)	7.49×10^{-7}	3.84×10^{-6}	3.9×10^{-7}	2.2×10^{-6}

[a] Calculated value by Lima's equation.

is written as the following equation [24]:

$$Q|_{r=r} = -\frac{2D_{\text{com}}}{rr_0}\sum_{n=1}^{\infty}(-1)^n \exp\left(-\frac{D_{\text{com}}n^2\pi^2 t}{r_0^2}\right)n\pi$$

$$\times \sin\left(\frac{n\pi r}{r_0}\right)\int_0^t \exp\left(-\frac{D_{\text{com}}n^2\pi^2\lambda}{r_0^2}\right)\phi(\lambda)\,d\lambda \quad (18)$$

Therefore, the amount of metal extracted in a unit mass of microcapsule, q, is derived as follows:

$$q = \frac{\int_0^{r_0} 4\pi r^2 \varepsilon_{\text{MC}} Q|_{r=r}\,dr}{4\pi r^3 \rho_{\text{MC}}/3} \quad (19)$$

where ρ_{MC} is the weight of the microcapsule per unit volume, and so $4\pi r^3 \rho_{\text{MC}}/3$ means the weight of a unit microcapsule. The ε_{MC} is pore density of a microcapsule. As shown above, the concentration of extracted complex at the surface, $\phi(t)$, is expressed as Eq. (16). Therefore, by substituting Eqs. (16) and (18) into Eq. (19), we can analytically calculate the relationship between q and t. The time course of the fractional attainment of equilibrium was calculated from Eq. (20), into which the calculated q values from Eq. (19) were substituted for each t value.

$$F(t) = \frac{q}{q^*} \quad (20)$$

where $F(t)$ means the fractional attainment of equilibrium and q^* means the equilibrium extraction amount of metal extracted into a unit mass of microcapsule. The q^* value can be calculated from the Langmuir extraction isotherm model.

4. Results and discussion

4.1. Extraction isotherms of lanthanides with microcapsules

Fig. 1(a) and (b) shows the extraction isotherms for lanthanum and samarium and erbium, respectively, at several pH values. These figures show that the extraction capacity for the metals was increased with increasing pH. Solid and broken lines in these figures correspond to lines calculated using the Lang-
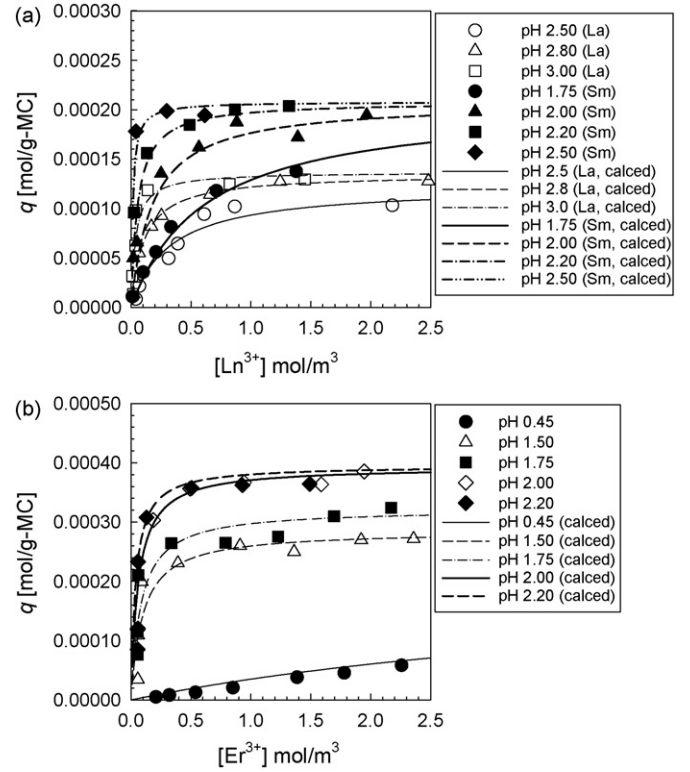

Fig. 1. Extraction isotherms for lanthanum, samarium and erbium with a microcapsule and calculated lines based on Langmuir model: (a) lanthanum and samarium; (b) erbium.

muir isothermal equation as shown in the following equation:

$$q^* = \frac{q_\infty K[\text{M}^{3+}]_{\text{aq}}}{1 + K[\text{M}^{3+}]_{\text{aq}}} \quad (21)$$

where q_∞ denotes the saturation amount of a metal extracted. K is the Langmuir constant. The determined q_∞ and K are listed in Table 4. As shown in Fig. 1, the calculated results correlate with the experimental data under all conditions. Therefore, q^* used for the calculation of $F(t)$ can be calculated from Eq. (21).

4.2. Extraction equilibria for liquid–liquid extraction system

The extraction equilibrium formula and the extraction equilibrium constants of some lanthanides under low EHPNA
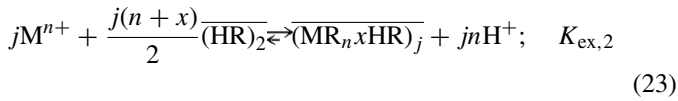
Table 4
Langmuir constants used to calculate q^*

pH	Lanthanum		Samarium		Erbium	
	q_∞ ($\times 10^{-4}$ mol/g MC)	K	q_∞ ($\times 10^{-4}$ mol/g MC)	K	q_∞ ($\times 10^{-4}$ mol/g MC)	K
0.45					2.20	0.19
1.5					2.85	10.2
1.75			2.08	1.63	3.22	12.0
2			2.08	5.59		
2.2			2.08	17.9		
2.5	1.23	3.15				
2.8	1.35	9.2				
3	1.37	27.0				

concentrations have been reported in the literatures [25,26]. The extraction of La, Nd and Er is expressed as follows:

$$\text{Ln}^{3+} + 3\overline{(\text{HR})_2} \rightleftarrows \overline{\text{LnR}_3 \cdot 3\text{HR}} + 3\text{H}^+; \quad K_{\text{ex},1} \tag{22}$$
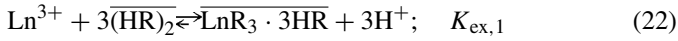
where over bar means the chemical species in the organic phase. $K_{\text{ex},1}$ denotes the overall extraction equilibrium constant under a low EHPNA concentration. The values of $K_{\text{ex},1} = 8.1 \times 10^{-3}$ (La), 8.2×10^{-2} (Nd) and 2.26×10^{-1} (Er). They were used to calculate the initial extraction rates of lanthanum, samarium and erbium under a low-extractant concentration by the above-mentioned interfacial reaction model.

As reported by Hino et al. [26], there is some possibility that the extraction equilibria of lanthanides with organophosphorus extractants are different at high loading, which occurs under conditions such as high pH and high-extractant concentration, than at low loading. Therefore, we investigated the extraction equilibrium formula of lanthanides with EHPNA under a high EHPNA concentration. The extraction equilibrium formula and the extraction equilibrium constants of lanthanum, samarium and erbium under a high EHPNA concentration were determined by analyzing the experimental data according to the slope analysis method shown below. The extraction equilibrium formula can be denoted by the following relationship:

$$j\text{M}^{n+} + \frac{j(n+x)}{2}\overline{(\text{HR})_2} \rightleftarrows \overline{(\text{MR}_n x\text{HR})_j} + jn\text{H}^+; \quad K_{\text{ex},2} \tag{23}$$

where $K_{\text{ex},2}$ is the extraction equilibrium constant at high loading. Eq. (23) is rewritten as Eqs. (24) and (25):

$$\log[(\text{MR}_n x\text{HR})_j]_{\text{org}} = j\log([\text{M}^{n+}]_{\text{aq}}[\text{H}^+]^{n^-})$$
$$+ \frac{j(n+x)}{2}\log[(\text{HR})_2]_{\text{org}} + \log K_{\text{ex},2} \tag{24}$$

$$\log[(\text{MR}_n x\text{HR})_j]_{\text{org}} - j\log([\text{M}^{n+}]_{\text{aq}}[\text{H}^+]^{n^-})$$
$$= \frac{j(n+x)}{2}\log[(\text{HR})_2]_{\text{org}} + \log K_{\text{ex},2} \tag{25}$$

The j value was determined by applying the relationship of Eq. (24) to the experimental data under the condition of the different pH and the same metal ion and extractant concentrations. It was determined as $j = 1$ for all metals investigated in this study (data not shown). The x value was determined by applying the relationship of Eq. (25) to the experimental data under the condition of the different extractant concentration and the same pH and metal ion concentration. Resultant plots for lanthanum, samarium and erbium show a linear relation (data not shown), and x and $K_{\text{ex},2}$ values for each metal were determined from the slope and the intercept of the straight lines. The extraction equilibrium constants are listed in Table 5, along with the determined extraction equilibrium formula. As shown in Table 5, the extraction equilibrium formula for lanthanides at high loading was different from that at low loading, as shown in Eq. (22). The formula was the same as that reported for Pr^{3+}, Nd^{3+}, Er^{3+} and Y^{3+} by Hino et al. [26]. The values of $K_{\text{ex},2}$ were used to calculate

Table 5
Extraction equilibrium equations and extraction equilibrium constants at high loading

Metal	Extraction equilibrium	$K_{\text{ex},2}$
La	$\text{La}^{3+} + \frac{5}{2}(\text{HR})_2 \rightleftarrows \text{LaR}_3 \cdot 2\text{HR} + 3\text{H}^+$	1.57×10^{-4}
Sm	$\text{Sm}^{3+} + \frac{5}{2}(\text{HR})_2 \rightleftarrows \text{SmR}_3 \cdot 2\text{HR} + 3\text{H}^+$	1.20×10^{-2}
Er	$\text{Er}^{3+} + \frac{5}{2}(\text{HR})_2 \rightleftarrows \text{ErR}_3 \cdot 2\text{HR} + 3\text{H}^+$	3.23

the initial extraction rates of lanthanum, samarium and erbium under a high-extractant concentration by the above-mentioned interfacial reaction model.

As shown in Eq. (22) and Table 5, under the same extractant concentration conditions, the extracted complexes of lanthanum, samarium and erbium have the same chemical formula. That is, the diffusion coefficients of the extracted complexes of each lanthanide can be regarded as almost identical under identical extractant concentration conditions. In other words, it is satisfactory to calculate the initial extraction rate of each lanthanide using the same diffusion coefficient expressed by Eqs. (13) and (14).

4.3. Determination of rate constants from the analysis for liquid–liquid extraction system

The initial extraction rate can be defined by the following equation:

$$R_{0,\text{SX}} = -\frac{V_{\text{aq}}}{A}\frac{d[\text{M}^{3+}]_{\text{aq}}}{dt}\bigg|_{t=0} = \frac{[\text{M}^{3+}]_{\text{aq},0}V_{\text{aq}}}{A}\frac{dE}{dt}\bigg|_{t=0} \tag{26}$$

where V_{aq} is the volume of the aqueous phase and A is the interfacial area. E is the extent of metal extracted.

Fig. 2(a) shows the relationship between the initial extraction rate, $R_{0,\text{SX}}$, and the extractant concentration. From the experimental data, it is clear that $R_{0,\text{SX}}$ increased with an increasing extractant concentration. The effects of pH and the initial concentration of each lanthanide on $R_{0,\text{SX}}$ are shown in Fig. 2(b) and (c), respectively. The solid and broken lines in Fig. 2 are the calculated results using the interfacial reaction model. In these figures, $K_{\text{ex},1}$ was used for the calculation. Other parameters used for the calculation are listed in Table 6. The rate constants of complex formation, k_1 and k_2, were evaluated by analyzing the experimental results with the interfacial reaction model. We determined the values of k_1 and k_2 with trial-and-error method. The obtained k_1 and k_2 are listed in Table 7. As shown in Fig. 2, close agreement between the experimental results and the calculated ones was obtained in all experiments. The agreement between the calculated lines and the experimental data indicates the suitability of the kinetic model used. Here, it should be noted that k_1 and k_2 were determined from the experimental data under a low-extractant concentration condition. In the next chapter, we try to simulate the initial extraction rate in the case of using undiluted EHPNA as the organic phase with the rate constants shown in Table 7. We also compare the calculated result for undiluted EHPNA and the experimentally obtained
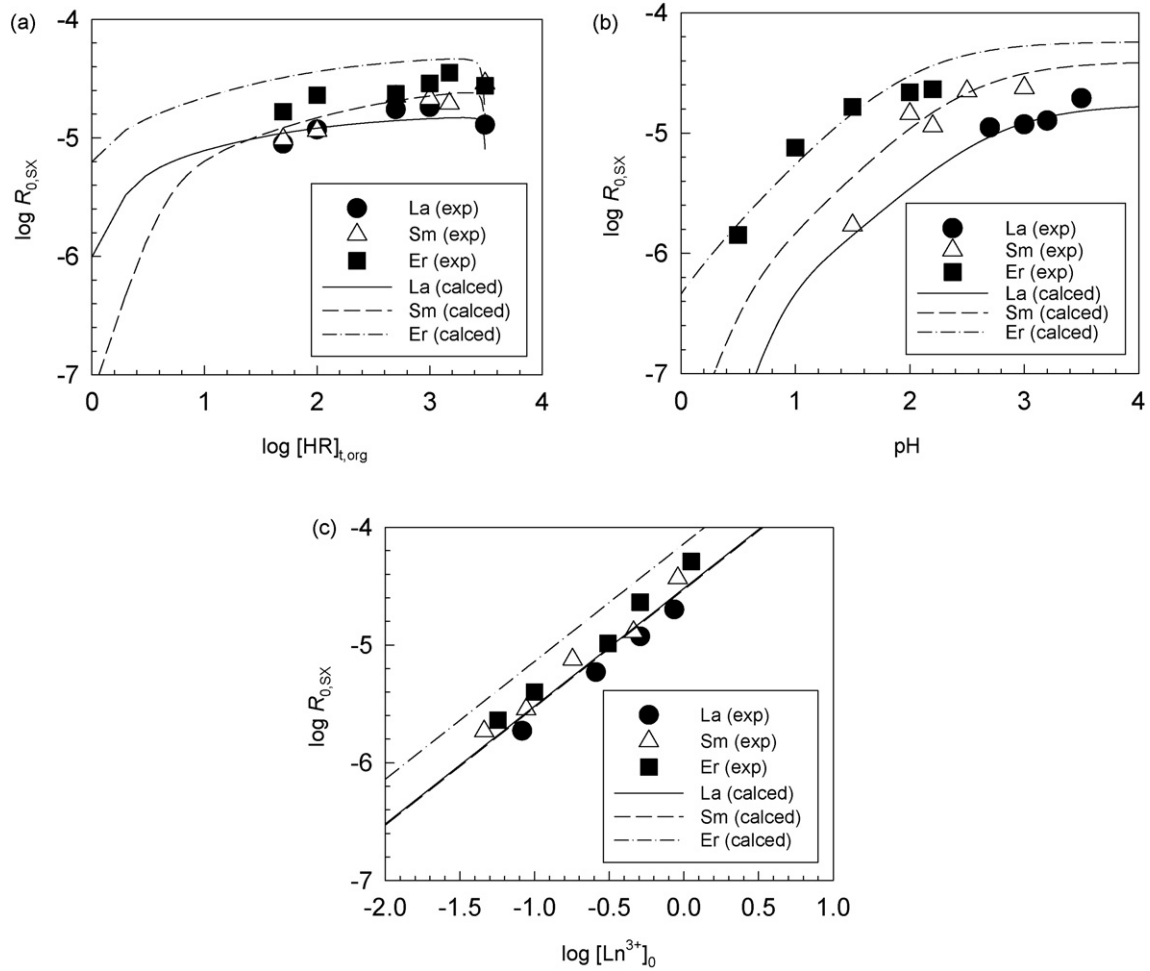
Fig. 2. Initial extraction rate for liquid–liquid extraction system. (a) Effect of extractant concentration, (b) effect of pH under diluted EHPNA condition and (c) effect of metal concentration under diluted EHPNA condition. Plots are experimental result. Lines are the calculated result.

Table 6
Values of constants for extraction of metals with EHPNA

Parameters	Value	Unit	Source
K_2	52	m^3/mol	[18]
K_a	7.9	mol/m^3	[18]
K_D	5.5×10^3		[18]
K_w	1.0×10^{-8}	$(mol/m^3)^2$	[31]
K_{HSO_4}	2.45×10^{-2}	m^3/mol	[31]
K_{MSO_4}	2.19 (for La); 1.82 (for Sm); 8.32×10^{-1} (for Er)	m^3/mol	[31]
K_{OH}	4.68×10^1 (for La); 2.45×10^2 (for Sm); 5.50×10^2 (for Er)	m^3/mol	[32]
δ_2	1×10^{-8}	m	[33]
δ_3	5×10^{-7}	m	[18]
k_M	1.4×10^{-4}	m/s	
ψ	1 (for SX system)[a]		[21]
	2 (for MC system)[b]		
V_1	322×10^{-6}	m^3/mol	[18]
I_1	1065		[18]
I_2	394		[18]
k	2.89		[18]
$K^*_{HR,org}$	2.5×10^{-1}	m^3/mol	[17]
$\Gamma^\infty_{HR,org}$	8.5×10^{-6}	mol/m^2	[17]

[a] SX system means liquid–liquid extraction system.
[b] MC system means microcapsule system.

initial extraction rate for the microcapsule system. In the microcapsules, the extractant exists in the undiluted state, because toluene used as a diluent in the preparation of the microcapsules would have evaporated from the microcapsules during polymerization [27]. The extractant concentration in the microcapsules is about 3100 mol/m³. The intraparticle diffusion resistance of the extracted complex may be significant for the microcapsule system. If the rate-determining step of extraction is the intraparticle diffusion step, the initial extraction rate for the microcapsule system is quite different from that for the above-mentioned liquid–liquid extraction system. On the other hand, if the complex formation reaction contributes to the rate-determining step of the extraction, the initial extraction rate for the microcapsule system can be explained by the interfacial reaction model by using the rate constants shown in Table 7.

Table 7
Kinetic constants obtained from the proposed model

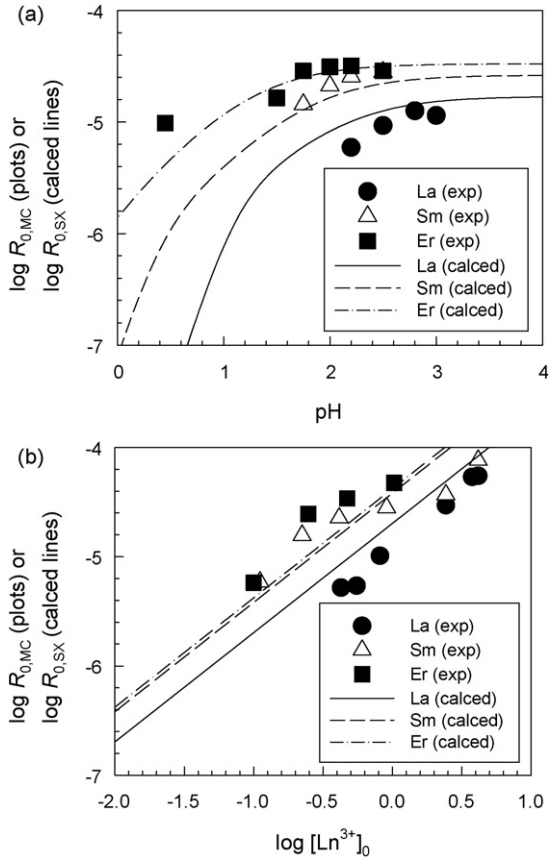| Metal	k_1 (m³/(mol s))	k_2 (m³/(mol s))
La	1.0	1.5×10^1
Sm	5.0×10^{-1}	4.5×10^1
Er	1.0×10^{-1}	1.9×10^2

Fig. 3. Initial extraction rate for microcapsule system. (a) Effect of pH under undiluted EHPNA condition and (b) effect of metal concentration under undiluted EHPNA condition. Plots are experimental result for microcapsule system. Solid and broken lines are the calculated results for liquid–liquid extraction system under undiluted EHPNA concentration.

4.4. Simulation of initial extraction rate of lanthanide ions into microcapsules

Plots in Fig. 3(a) and (b) show the effect of pH and metal concentration on the initial extraction rate of the microcapsule system, $R_{0,MC}$, respectively. $R_{0,MC}$ values were calculated using the slopes of the uptake curves during the early periods of the extractions. They were calculated according to the following equation:

$$R_{0,MC} = \frac{m}{A_{MC}} \frac{dq}{dt}\bigg|_{t=0} = \frac{q^* m}{A_{MC}} \frac{dF(t)}{dt}\bigg|_{t=0} \qquad (27)$$

where m and A_{MC} are the amount and the effective surface area of microcapsules packed in the shallow bed, respectively. In this study, A_{MC} was calculated by using a spherical surface area with an average radius of the microcapsule, because it can be regarded that EHPNA is present at the surface of the microcapsule as well as in the microcapsule. EHPNA has interfacial activity [28], and it adsorbs on the interface between the continuous aqueous phase and the dispersed organic phase when a microcapsule is formed. Divinylbenzene in the dispersed phase is polymerized in situ [17,27], therefore a monomolecular layer of EHPNA would be formed on the surface of a microcapsule. As shown in the plots in Fig. 3, the relationships between log

$R_{0,MC}$ and pH and between $R_{0,MC}$ and the initial metal concentration show the same tendencies as the relationships shown in Fig. 2(b) and (c), respectively.

The solid and broken lines shown in Fig. 3 are the calculated results for undiluted EHPNA according to Eq. (1). In the calculation, the extractant concentration was changed from 100 to $3100\,mol/m^3$. The rate constants used for the calculation were determined under a low EHPNA concentration and are shown in Table 7. The $K_{ex,2}$ values shown in Table 5 were used for the calculation. The other parameters are listed in Table 6. As shown in Fig. 3, reasonable agreement between $R_{0,MC}$ and $R_{0,SX}$ for undiluted EHPNA was obtained in all experiments. That is to say, it is considered that the complex formation reaction at the surface of the microcapsule strongly contributes to the rate-determining step of extraction for the microcapsule system. Therefore, the rate constants of the complex formation reaction, k_1 and k_2, are the key parameters for analyzing the extraction uptakes of lanthanides into the microcapsule. It is expected that the uptakes of lanthanides by the microcapsule can be simulated using the rate constants determined for a liquid–liquid extraction system with a low EHPNA concentration.

4.5. Prediction of uptake curves of lanthanides into microcapsule

The uptake curves for lanthanum, samarium and erbium are shown in Figs. 4–6, respectively. The effects of the metal concentration and the pH in the aqueous solution on lanthanum, samarium and erbium extraction are shown in Figs. 4(a) and (b), 5(a) and (b) and 6(a) and (b), respectively.
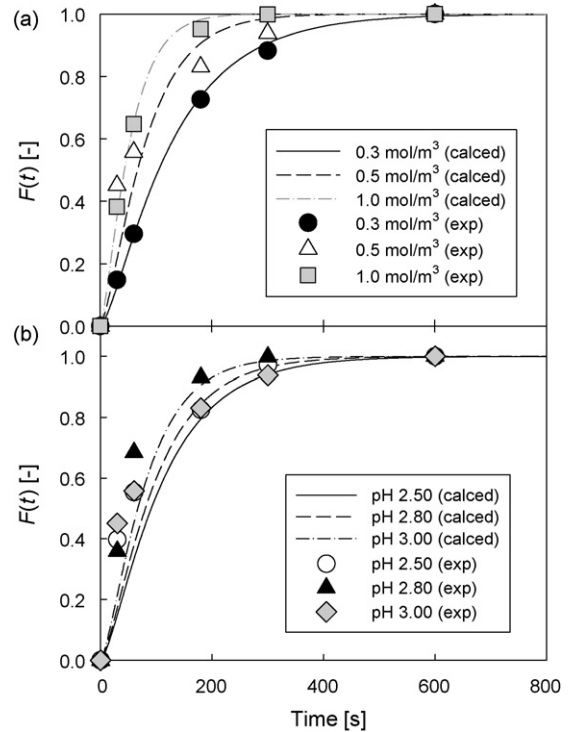

Fig. 4. Uptake curves of lanthanum extraction for various metal concentrations (a) and pHs (b). Solid and broken lines are the calculated results based on the proposed model.
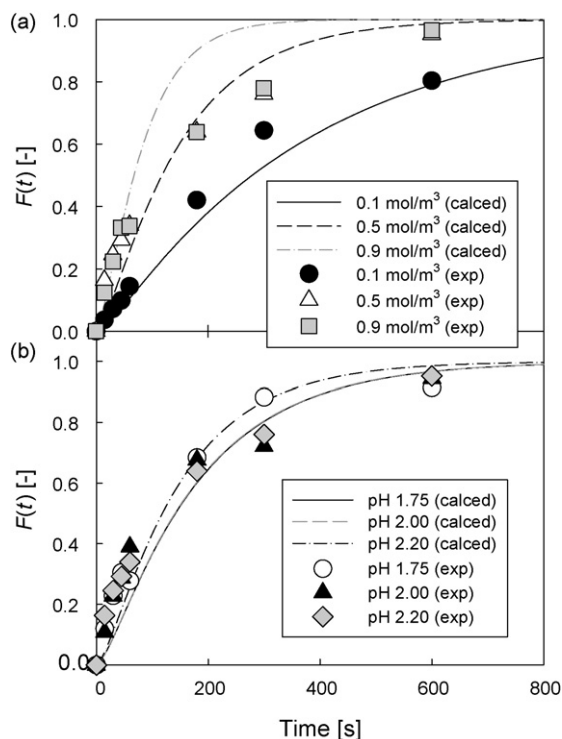
Fig. 5. Uptake curves of samarium extraction for various metal concentrations (a) and pHs (b). Solid and broken lines are the calculated results based on the proposed model.
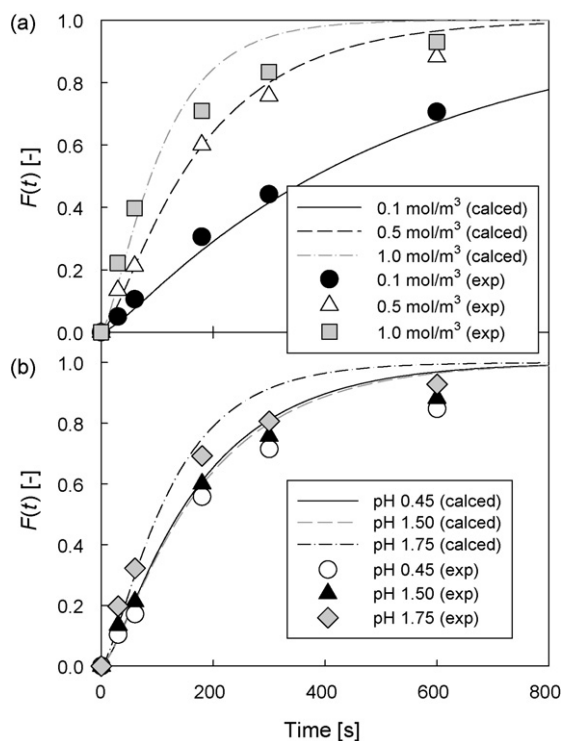

Fig. 6. Uptake curves of erbium extraction for various metal concentrations (a) and pHs (b). Solid and broken lines are the calculated results based on the proposed model.

The plots in Figs. 4(a), 5(a) and 6(a) clearly indicate that the higher the metal concentration in the aqueous phase, the faster $F(t)$ reaches 1. That is, the extraction rate quickened as the metal concentration in the aqueous phase increased. In addition, as shown in the plots in Figs. 4(b), 5(b) and 6(b), no significant difference between the uptake curves for different pH was observed for the three metals investigated. These results indicate that the extraction rate depends on the metal concentration but not the pH of the aqueous phase under the experimental conditions investigated in this study. These tendencies of the extraction rate are reasonable, i.e. the initial extraction rates shown in Fig. 3(a) indicate the same tendencies for the corresponding pH ranges.

We tried to simulate the uptakes with the kinetic model for the microcapsule extraction derived in Section 3.2. In the calculation, parameters shown in Tables 1–7 were used. In Figs. 4–6, solid and broken lines show the calculated results obtained with the kinetic model. As indicated in these figures, the calculated uptake curves correspond well to almost all the experimental data, except for samarium and erbium extraction at $t > 200$ s under a high metal concentration. The calculated results explain the extraction tendencies resulting from variations in the metal concentration and the pH. That is to say, the calculated uptakes increased with an increasing the metal concentration, but are independent of pH. From these results, it is suggested that the proposed kinetic model is adequate for the metal extraction system with the microcapsules. We can predict the extraction uptakes of lanthanides with microcapsules containing EHPNA by using the theoretical model based on the interfacial reaction model accompanied with the intraparticle diffusion as expressed by Fick's law and the complex formation rate constants determined for a liquid–liquid extraction system.

In the cases of high metal concentrations for samarium (0.9 mol/m³) and erbium (1.0 mol/m³) extraction, for which the data are shown in Figs. 5(a) and 6(a), the calculated results deviate from the experimental data with increasing time. This disagreement was considered to occur as a result of the pore closing at the surface of the microcapsule due to the condensate of the extracted complex, which appears as a third phase in the liquid–liquid extraction system. Namely, in the case of extraction of metals like samarium and erbium, which have both a fast complex formation rate and a strong affinity to EHPNA, it is suggested that variation of the effective intraparticle diffusion coefficient with the metal concentration in an aqueous phase, which has been reported for extraction systems with solvent-impregnated resins by Cortina et al. [29] and Serarols et al. [30], would result from the shrinkage of the pore radius due to the increase in the amount of extracted condensate. The same phenomenon was found in the uptake curve for indium extraction reported in the previous paper [16].

5. Conclusion

In this study, we investigated the extraction kinetics behaviors of lanthanum, samarium and erbium with a microcapsule containing EHPNA. The initial extraction rates of lanthanides in the microcapsule system were affected by the external aqueous conditions, such as the pH and metal concentration. It was

found that the initial extraction rate for the microcapsule system varied in the same way with pH and metal concentration as it does in a liquid–liquid extraction system. The initial extraction rate for a liquid–liquid extraction system at low loading was analyzed and the rate constants of the complex formation reaction were determined. By using the determined rate constants, the initial extraction rate for a liquid–liquid extraction system at high loading was predicted. From the comparison between the experimentally obtained initial extraction rate for the microcapsule system and the calculated initial extraction rate at high loading, it was found that the initial extraction rate for the microcapsule system was almost the same as the initial extraction rate calculated when undiluted EHPNA was used as the organic phase. With the determined rate constants, the uptake curves of lanthanides into microcapsules containing EHPNA were predicted. A theoretical model which was derived from the liquid–liquid interfacial complex formation reaction following intraparticle diffusion was used for the prediction of the uptakes. The calculated results predicted the variation in the extraction rate with changes in the metal concentration and the pH in the aqueous phase well. As the result of the present study, the extraction of metal ion with the microcapsule was successfully predicted by using the rate constant determined for the usual liquid–liquid extraction system. That is to say, if we have the knowledge of extraction dynamics for the usual liquid–liquid extraction, we instantly predict the extraction rate for the microcapsule system.

Acknowledgment

References

[1] H. Small, Gel liquid extraction. The extraction and separation of some metal salts using tri-*n*-butyl phosphate gels, J. Inorg. Nucl. Chem. 18 (1961) 232–240.

[2] Y. Wakui, H. Matsunaga, T.M. Suzuki, Distribution of rare earth elements between (2-ethylhexyl hydrogen 2-ethylhexylphosphonate)-impregnated resin and acid aqueous solution, Anal. Sci. 4 (1988) 325–327.

[3] M. Yoshida, K. Uezu, F. Nakashio, M. Goto, Spacer effect of novel bifunctional organophosphorus monomers in metal-imprinted polymers prepared by surface template polymerization, J. Polym. Sci. A 36 (1998) 2727–2734.

[4] M. Yoshida, K. Uezu, M. Goto, S. Furusaki, Metal ion imprinted microsphere prepared by surface molecular imprinting technique using water-in-oil-in-water emulsions, J. Appl. Polym. Sci. 73 (1999) 1223–1230.

[5] K. Araki, M. Yoshida, K. Uezu, M. Goto, S. Furusaki, Lanthanide-imprinted resins prepared by surface template polymerization, J. Chem. Eng. Jpn. 33 (2000) 665–668.

[6] K. Takeshita, Y. Takashima, S. Matsumoto, H. Yamanaka, Extraction of cerium(III) by polymer gels swollen with bidentate organophosphorus compounds, J. Chem. Eng. Jpn. 28 (1995) 91–96.

[7] K. Takashita, M. Kumagai, Y. Takashima, S. Matsomoto, Extraction of cerium(III) by solid extractant impregnated with dihexyl-*N,N*-diethylcarbamoylmethylphosphonate, J. Chem. Eng. Jpn. 27 (1994) 52–56.

[8] Y. Wakui, H. Matsunaga, T.M. Suzuki, Selective recovery of trace scandium from acid aqueous solution with (2-ethylhexyl hydrogen 2-ethylhexylphosphonate)-impregnated resin, Anal. Sci. 5 (1989) 189–193.

[9] H. Matsunaga, A.A. Ismail, Y. Wakui, T. Yokoyama, Extraction of rare earth elements with 2-ethylhexyl hydrogen 2-ethylhexyl phosphonate impreg-

[10] C. Gok, S. Seyhan, M. Merdivan, M. Yurdakoc, Separation and preconcentration of La^{3+}, Ce^{3+} and Y^{3+} using calix[4]resorcinarene impregnated on polymeric support, Microchim. Acta 157 (2007) 13–19.

[11] V.K. Jain, A. Handa, R. Pandya, P. Shrivastav, Y.K. Agrawal, Polymer supported calix[4]arene-semicarbazone derivative for separation and pre-concentration of La(III), Ce(III), Th(IV) and U(VI), React. Funct. Polym. 51 (2002) 101–110.

[12] V.K. Jain, A. Handa, S.S. Sait, P. Shrivastav, Y.K. Agrawal, Pre-concentration, separation and trace determination of lanthanum(III), cerium(III), thorium(IV) and uranium(VI) on polymer supported *O*-vanillinsemicarbazone, Anal. Chim. Acta 429 (2001) 237–246.

[13] S. Nishihama, N. Sakaguchi, T. Hirai, I. Komasawa, Extraction and separation of rare-earth metals using microcapsules containing bis-(2-ethylhexyl)phosphoric acid, Hydrometallurgy 64 (2002) 35–42.

[14] E. Kamio, K. Kondo, Separation and concentration of lanthanoids using microcapsules containing acidic organophosphorus compounds as an extractant, J. Chem. Eng. Jpn. 35 (2002) 574–581.

[15] E. Kamio, M. Matsumoto, F. Valenzuela, K. Kondo, Sorption behavior of Ga(III) and In(III) into a microcapsule containing long-chain alkylphosphonic acid monoester, Ind. Eng. Chem. Res. 44 (2005) 2266–2272.

[16] E. Kamio, M. Matsumoto, K. Kondo, Theoretical development of metal extraction mechanism into an extractant-impregnated microcapsule, Ind. Eng. Chem. Res. 46 (2007) 255–265.

[17] E. Kamio, M. Matsumoto, K. Kondo, Extraction mechanism of rare metals with microcapsules containing organophosphorus compounds, J. Chem. Eng. Jpn. 35 (2002) 178–185.

[18] E. Kamio, H. Miura, M. Matsumoto, K. Kondo, Extraction mechanism of metal ions on the interface between aqueous and organic phases at a high concentration of organophosphorus extractant, Ind. Eng. Chem. Res. 45 (2006) 1105–1112.

[19] H. Matsuyama, Y. Miyake, Y. Izumo, M. Teramoto, Kinetics and mechanism of metal extraction with acidic organophosphorus extractants. II. Extraction mechanism of Fe(III) with di(2-ethylhexyl) phosphoric acid, Hydrometallurgy 24 (1990) 37–51.

[20] C.R. Wilke, P. Chang, Correlation of diffusion coefficient in dilute solutions, AIChE J. 1 (1955) 264–270.

[21] M. Souders Jr., Viscosity and chemical constitution, J. Am. Chem. Soc. 60 (1938) 154–158.

[22] F.W. Lima, On the viscosity of binary liquid mixtures, J. Phys. Chem. 56 (1952) 1052–1054.

[23] P. Chang, C.R. Wilke, Some measurements of diffusion in liquids, J. Phys. Chem. 59 (1955) 592–596.

[24] J. Clank, The Mathematics of Diffusion, 2nd ed., Oxford Science Publishers, Great Britain, 1975.

[25] M. Goto, T. Kakoi, N. Yoshii, K. Kondo, F. Nakashio, Effect of synthesized surfactants in the separation of rare earth metals by liquid surfactant membranes, Ind. Eng. Chem. Res. 32 (1993) 1681–1685.

[26] A. Hino, S. Nishihama, T. Hirai, I. Komasawa, Practical study of liquid–liquid extraction process for separation of rare earth elements with bis(2-ethylhexyl)phosphinic acid, J. Chem. Eng. Jpn. 30 (1997) 1040–1046.

[27] H. Yoshizawa, K. Fujikubo, Y. Uemura, Y. Kawano, K. Kondo, Y. Hatate, Preparation of divinylbenzene homopolymeric microcapsules with highly porous membranes by in situ polymerization with solvent evaporation, J. Chem. Eng. Jpn. 28 (1995) 78–84.

[28] Y. Sato, Y. Akiyoshi, K. Kondo, F. Nakashio, Extraction kinetics of copper with 2-ethylhexylphosphonic acid mono-2-ethylhexyl ester, J. Chem. Eng. Jpn. 22 (1989) 182–189.

[29] J.L. Cortina, R. Arad-Yellin, N. Miralles, A.M. Sastre, A. Warshawsky, Kinetics studies on heavy metal ions extraction by Amberlite XAD2 impregnated resins containing a bifunctional organophosphorous extractant, React. Funct. Polym. 38 (1998) 269–278.

[30] J. Serarols, J. Poch, M.F. Llop, I. Villaescusa, Determination of the effective diffusion coefficient for gold(III) on a macroporous resin XAD-2 impregnated with triisobutyl phosphine sulfide, React. Funct. Polym. 41 (1999) 27–35.

nated resins having different morphology and reagent content, React. Funct. Polym. 49 (2001) 189–195.

[31] L.G. Sillén, A.E. Martell, Stability Constants of Metal–Ion Complexes. Supplement no. 1. Dedicated to the Memory of Lars Gunnar Sillen. Part I. Inorganic Ligands. Compiled by Lars Gunnar Sillén. Part II. Organic Including Macromolecule Ligands. Compiled by Arthur E. Martell, Alden Press, London, 1971.

[32] R.M. Smith, A.E. Martell, Critical Stability Constants, vol. 4, Plenum Press, New York, 1976.

[33] S. Ishizaka, N. Kitamura, Time-resolved total internal reflection fluorometry study on chemical and structural characteristics at water/oil interface, Bull. Chem. Soc. Jpn. 74 (2001) 1983–1998.